

Exploring Causes of Representational Similarity in Machine Learning Models

Zeyu Michael Li*, Hung Anh Vu*, Damilola Awofisayo, Emily Wenger

Department of Electrical and Computer Engineering

Duke University, Durham NC

{zeyu.li030, hung.vu, dami.awofisayo, emily.wenger}@duke.edu

Abstract

Numerous works have noted significant similarities in how machine learning models represent the world, even across modalities. Although much effort has been devoted to uncovering properties and metrics on which these models align, surprisingly little work has explored causes of this similarity. To advance this line of inquiry, this work explores how two possible causal factors—dataset overlap and task overlap—influence downstream model similarity. The exploration of dataset overlap is motivated by the reality that large-scale generative AI models are often trained on overlapping datasets of scraped internet data, while the exploration of task overlap seeks to substantiate claims from a recent work, the Platonic Representation Hypothesis, that task similarity may drive model similarity. We evaluate the effects of both factors through a broad set of experiments. We find that both positively correlate with higher representational similarity and that combining them provides the strongest effect. Our code[†] and dataset[‡] are published.

1 Introduction

AI models can now classify images, generate text, and create content with high accuracy and fidelity. Consequently, they are used in numerous industries, from national security [62, 5] to healthcare [33, 56]. Given our increasing dependence on AI models in these critical areas, it is critical to interrogate properties of these models and understand their capabilities and limits.

One interesting, well-studied phenomenon is representational similarity across AI models. A large body of work has considered ways in which AI model representations (e.g. their mathematical depictions of real-world inputs) align. Although much of this work has focused on neural networks, recent work has applied similar methods to generative models like large language models (LLMs) and found some evidence of “feature universality” across these models [22].

Although representational alignment is well-documented and novel methods for measuring it are developed frequently, we still do not understand why it happens. Only a few prior works have addressed this question empirically, proposing loss function similarity [45] or inductive bias as possible causal factors [59]. Recent work [22] postulated that *task alignment* among large-scale AI models will increase their similarity, since as models grow larger they will perform more tasks, and this set of tasks will eventually converge. While compelling, this argument lacks empirical evidence.

We believe another, unexplored factor could also drive model alignment: *dataset overlap*. Many of today’s massive generative AI models, such as Meta’s LLaMA, Open AI’s ChatGPT, and Google’s Gemini, are trained on huge swaths of the internet. This design choice follows well-established

*These authors contributed equally and are ordered alphabetically by last name.

[†]<https://github.com/lizeyu090312/ReprSimCauses>

[‡]<https://kaggle.com/datasets/6482c94477918953cec99b03f1330d3afc679e8be2b35113b2463c5688389c18>

scaling laws in the AI community, which state that training on more data produces a better model. While massive and relatively cheap to acquire, internet-sourced model training datasets may overlap significantly. For example, many models are trained on subsets of Common Crawl, a massive dataset composed of most of the internet. Many are also trained on Reddit, Wikipedia, and other “known” sources of relatively high quality internet data [42, 3]. It seems not-unreasonable that overlap in training datasets could drive downstream model similarity.

Since limited work explores causes of representational similarity, these two competing hypotheses for model alignment remain unexplored. The *task alignment* hypothesis of [22] is only ever argued-for theoretically, so no experiments exist. Similarly, the *dataset overlap* hypothesis not been explored, since the AI research community focuses more on issues of privacy and copyright in large-scale internet data use, not downstream effects on model behaviors.

Our contribution. We propose empirical methods to explore of causes of representational similarity. Building on hypotheses of prior work [22] and known realities of model training, we focus specifically on measuring the effects of dataset overlap and task alignment on representation similarity. To do this, we propose two novel methods, *dataset splitting* and *task splitting*, for generating training datasets that control overlap at both the data point and task level, allowing us to quantify how much overlap on these properties affects representation similarity. Along the way, we create a new dataset, called ColorShapeDigit800K, to train models with nuanced task differences, which will be open-sourced upon publication of our paper. We run dataset and task splitting experiments on models ranging from classifiers to small language models and find that:

- **Both dataset and task overlap are positively correlated with increased representational similarity in models.** We observe this trend in nearly all models and datasets we evaluate, from image classifiers to VAEs to text generation models.
- **Increasing dataset and task overlap together induces strongest representational alignment between models, as measured by mutual information.** We compare the mutual information between different overlap types and measured representational similarity in models.

The rest of the paper proceeds as follows. §2 situates our study in the broader landscape of work on representational similarity. §3 motivates the two causal factors we explore—dataset and task overlap. §4 provides details on our experimental setup, while §5 presents our key findings. §6 discusses limitations and broader impacts of our work.

2 Related Work

Observations of model similarity. Numerous prior works have demonstrated that machine learning models, even those trained for different tasks, can exhibit similar properties [34, 44, 50, 29, 31, 21, 57], either in their outputs (*functional* similarity) or their internal behaviors (*representational* similarity, the focus of this work). Prior work on representational similarity has considered similarities in neuron activation patterns [14, 17] and feature space representations of inputs [31, 21, 44], and numerous metrics have been proposed to measure similarities between models [29, 28, 22, 36, 16, 18, 2, 37, 21]. Extensions of this phenomenon, including alignment between AI model and human representations of the world, is an ongoing area of research (see [57] for a detailed overview).

Causes of model similarity. Prior work has explored factors affecting similarity of computer vision models, such as increases in model and dataset size [29, 52, 22], overall training objectives [8, 32], multi-modality task generalization [22], and model initialization [34]. The main findings show that alignment scales with model and dataset size and that differences in training objective and tasks cause divergent model representations [57]. However, these factors have only been explored at a high level, and little attention has been devoted to untangling direct *causes* of representational similarity in models. This motivates our work, which empirically studies how two possible causal factors—dataset overlap and task overlap—affect representational similarity.

Downstream effects of representational similarity. Beyond curiosity about causes of model similarity, our work is motivated by concerns about negative effects of unexpected model similarity. Sometimes, similarity is desired and explicitly constructed—e.g. via techniques like model distillation and transfer learning that explicitly pass knowledge from one model to another to expedite learning [48, 6, 57, 54, 11]. However, representation alignment between models may not always be desirable. For example, Wenger and Kenett [63] showed that large language models exhibit

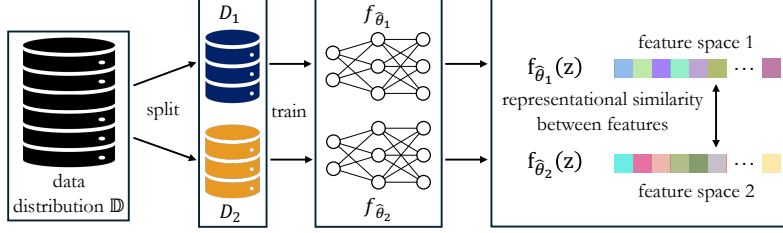


Figure 1: **Overview of our experimental framework.** Two models are trained on dataset splits with controlled dataset or task overlap, and we measure their representational similarity.

homogeneous behaviors on creative tasks. If independently trained models converge to similar representations, their resulting behavior could limit diversity in downstream applications and cause pervasive bias or consistent errors across models. There are numerous applications also in which model diversity matters, such as ensemble learning [38, 64] or multi-agent systems [19]. We believe that studying *causes* of representational similarity across models could reveal mitigation strategies to address unwanted model convergence.

3 Setup and Intuition

In this work, we consider two models, $f_{\hat{\theta}_1}$ and $f_{\hat{\theta}_2}$, trained on datasets D_1 and D_2 respectively. Each dataset consists of samples drawn from an unknown true data distribution \mathbb{D} . Each model is optimized to minimize a loss function on samples from their respective datasets:

$$\hat{\theta}_i = \arg \min_{\theta} \mathbb{E}_{(z,y) \in D_i} [\mathcal{L}(h_{\theta}(f_{\theta}(z)), y)] \quad (1)$$

where \mathcal{L} is the training objective. The model consists of f and h parameterized by $\hat{\theta}_i$, where f is the backbone that generates a rich latent-space representation of input z and h is a small head module that transforms the latent vector into human-usable outputs, perhaps classification decisions or generated text. In this work, we are interested in the output of f , where $f_{\hat{\theta}_i} : \mathbb{D} \rightarrow \mathbb{R}^n$ maps an input $z \in \mathbb{D}$ to an n -dimensional latent representation of input z . Given an input $z \in \mathbb{D}$ and model backbones $f_{\hat{\theta}_1}$ and $f_{\hat{\theta}_2}$, we can measure the similarity in the latent representations of $f_{\hat{\theta}_1}(z)$ and $f_{\hat{\theta}_2}(z)$. Figure 1 provides an overview of this end-to-end framework, which forms the backbone of our methodology.

Numerous prior works have measured similarities between $f_{\hat{\theta}_1}$ and $f_{\hat{\theta}_2}$. However, little work has explored *causes* of such similarities. In this work, we propose to study the relative effects of two potential causes on downstream representational similarity: dataset overlap and task overlap. Given the wide open nature of this line of inquiry, we believe that focusing on two potential causes is sufficient. Future work should rigorously examine additional causal factors.

3.1 Dataset overlap

Our exploration of this factor is motivated by the reality that today’s large-scale AI models are trained on overlapping datasets. Due to ever-increasing demands for training data [23], model trainers often turn to internet scrapes as a rich and cheap source of data. From whitepapers, one can easily discern that the scraped training dataset of large models often overlap. For example, GPT [4], Jamba [58], Llama [60], PaLM [7], and Phi [1] are all trained on subsets of CommonCrawl [10], while GPT, Llama, and PaLM are all trained on Wikipedia and Books datasets. This reality motivates our exploration of how *dataset overlap* drives downstream representational similarity.

Intuitively, a large amount of overlapping content in training datasets D_1 and D_2 (both drawn from the same underlying data distribution \mathbb{D}) should lead to high similarity in latent representations produced by the two models. Suppose two datasets overlap significantly, i.e., $D_1 \cap D_2 \approx D_1 \cup D_2$, then solving Equation (1) for D_1 and D_2 produces models optimized toward the similar underlying input-label patterns in the two datasets. As a result, the backbones should output similar latent representations for the same data. Prior work shows that models trained on disjoint datasets drawn from the same true distribution (e.g. face images) also exhibit significant similarity in latent space representations [55], increasing our confidence in this hypothesis.

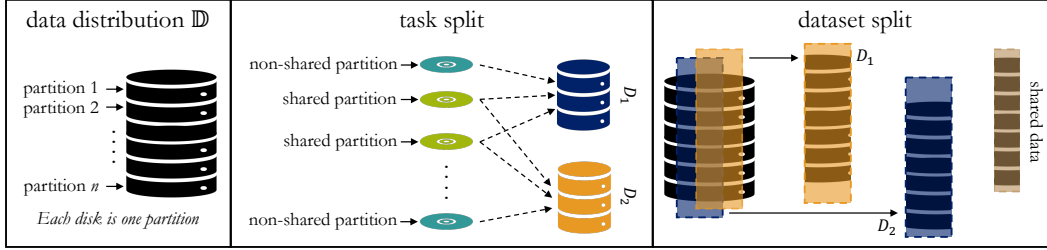


Figure 2: **Our task and dataset splitting strategies.** Task splitting organizes partitions (e.g. classes in image datasets or text data with a specific style) in the original dataset into two new datasets. Dataset splitting produces new datasets with certain amounts of per-class overlap.

3.2 Task overlap

Prior work speculates that overlap in model tasks, e.g. specific desired model behaviors, will increase downstream model similarity ([22], Section 3.1). Intuitively, this makes sense: two models trained to answer science and math questions will likely be more similar than a model trained to answer science and math questions and a model trained for general-purpose text completion. However, the claims of [22] are not explored empirically. This motivates our quantitative exploration of *task overlap* as a second potential cause of representational similarity.

In our work, we define a model task as a *specific type of data that the model is trained to process within a fixed learning paradigm* (e.g. supervised learning, self-supervised learning). For example, each class in the CIFAR-10 dataset constitutes a task; in a similar vein, next token prediction on the Shakespeare and Tiny-Codes datasets are two distinct tasks. Our key insight in evaluating task overlap is that a single training data element can be used for multiple learning tasks based on how it is labeled. For example, in computer vision, an image containing both a digit and shape can be used to train one model to recognize digits and another to recognize shapes. Similarly, in language models, the same sequence of text can be used to generate text in different styles. Within the same learning paradigm, the underlying data remains the same, but the task partition determines the type of representation the model learns by assigning different objectives to the same or overlapping datapoints. We leverage this insight to design our task overlap experiments.

4 Methodology

To test the relative effects of dataset and task overlap on downstream representational similarity, we trained numerous models with varying data and task overlap in their training datasets. This section describes the techniques used to induce dataset and task overlap and methods for model training and evaluation. Figure 2 gives an overview of our task and dataset splitting approaches.

4.1 Dataset overlap

We split datasets by dividing up data points in each partition and fixing a certain amount of partition-level data point overlap between models. Practically, this means we consider two datasets D_1 and D_2 , each containing data points drawn from the same set of partitions (e.g. classes in image classification). Given a fixed overlap proportion $\alpha \in [0, 1]$, we modify the data points in each partition such that for every partition p , a proportion α of the data points in D_1 and D_2 are shared (i.e., identical), and the remaining proportion $1 - \alpha$ of data points are unique to each dataset. This ensures that each partition in D_1 and D_2 has an exact overlap proportion of α .

4.2 Task overlap

Task splitting with varying dataset overlap. Defining task similarity requires varying the *training objective* rather than the data points seen during training. For our baseline approach, we control task similarity between models trained on otherwise-identical datasets D_1 and D_2 by varying the number of overlapping partitions p between the two datasets. Specifically, we split the data into partitions $P = \{p_0, p_1, \dots, p_n\}$, where each partition corresponds to a class (or, in the case of

language datasets, tokens from different corpora). We construct D_1 and D_2 by selecting K total partitions for each, with αK partitions shared between them and $(1 - \alpha)K$ partitions unique to each.

Task splitting varies the training objective between datasets D_1 and D_2 by controlling the number of shared partitions (α), unlike dataset splitting which shares data points directly. As α decreases, the models train on increasingly different subsets of the original dataset \mathbb{D} , potentially influencing their representation similarity. However, since dataset partitions contain distinct data points, increasing overlap in partitions also increases the amount of shared training data, making it hard to isolate the effect of task similarity from data overlap. To address this, the next section introduces a task splitting approach where partition overlap is varied but data overlap is constant.

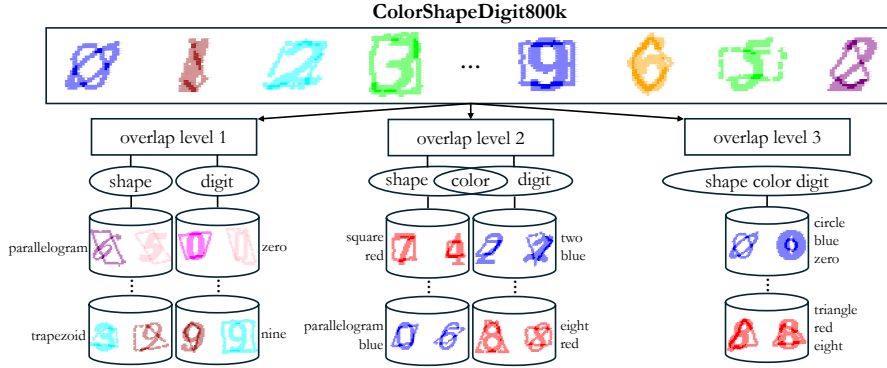


Figure 3: **Illustration of dataset pairs with different levels of task overlap.** Datasets with varying levels of task overlap (they all share the same images). The task overlap progressively increases from left to right. Example images and the corresponding labels are shown for each dataset at a particular task overlap.

Task splitting with constant dataset overlap. We construct a new dataset, ColorShapeDigit800K, which maintains a fixed set of data points while varying the task definition. This approach allows us to control training objective similarity simply by modifying dataset labels. ColorShapeDigit800K is constructed from two datasets: geometric shape images from [51] and digit images from [24]. We choose these base datasets because both contain large collections of visually simple and distinct shapes and digits on clean backgrounds, which enable compositional task construction. More complex data with noisier backgrounds would make it more difficult to control task-specific features.

Table 1: **Composition of dataset pairs in ColorShapeDigit800K.** The labels of D_1 , D_2 and the number of classes in D_1 , D_2 for each level of task overlap is provided as $\langle \text{info for } D_1 \rangle / \langle \text{info for } D_2 \rangle$. S, D, and C refer to shape, digit, and color, respectively. Figure 6 combines levels 2A, 2B, and 2C.

Overlap level	1	2A	2B	2C	3
Labels	S/D	S+D/S+C	S+D/D+C	S+C/D+C	S+D+C/S+D+C
Number of classes	8/10	80/80	80/100	80/100	800/800

For our experiments with this task overlap approach, we use identical data points in both D_1 and D_2 and progressively adjust the labelling scheme to define increasingly specific tasks (e.g., based on shape, digit, or color). This is illustrated in Figure 3. As more attributes are incorporated into the task definition, the training objectives across D_1 and D_2 become more aligned, although the data points never change. This progression of the labelling scheme to consider more attributes is summarized in Table 1, which shows how the complexity in the number of classes increases as more attributes are considered. At the extreme, when all data attributes are used in labelling, the models are trained on identical tasks. This approach allows us to examine how increasing task similarity affects model representations but avoids the confounding variable of increasing dataset overlap. The downside of this approach is that it leverages a different dataset than that used in our dataset overlap and baseline task overlap experiments, potentially rendering results less comparable.

4.3 Experimental setup

We run our task and dataset splitting experiments on a variety of settings. This section describes the basic model setup and how we evaluate representational similarity, then gives details about how we implement the different splitting approaches.

Model training. Table 2 provides an overview of the models used in our experiments. To understand how our different overlap approaches affect representational similarity across modalities, we train image classifiers, variational autoencoders (VAEs), and small language models. We trained all models using similar hardware setup (Single NVIDIA RTX 6000 Ada Generation GPU). For the ResNet-18 models we leverage the FFCV library for accelerated data loading. All ResNet models used cross entropy loss with label smoothing at 0.1. The VAE leveraged a singular encoder and decoder with composite generative loss. The language models are a GPT-Style transformer [25] with optimizations such as mixed precision, gradient accumulation & clipping, and early stopping, with task overlap and/or data overlap varied across runs. In the Appendix, Table 4 gives full hyperparameter details, while Table 5 lists baseline model performance.

Table 2: **Models and datasets used in our experiments.** * = *ColorShapeDigit800K* was only used to train a ResNet18 model for task overlap experiments; all other models/datasets were used for both task and dataset overlap experiments.

Models	Training Data	Overlap Methods Dataset Task	
ResNet18 [20]	CIFAR-10 [30], CIFAR-100 [30] TinyImagenet [12], ColorShapeDigit800K* (ours)	✓	✓*
VAE [26]	CIFAR-10 [30]	✓	✓
nanoGPT [25]	Tiny-{Stories, Codes} [15, 40], Shakespeare [9], Tiny-{WebText, TextBooks} [41, 39], WikiText [35]	✓	✓

Measuring representational similarity. After training, we evaluate the downstream effects of the various overlap methods by measuring the representational similarity between pairs of models trained with a specific dataset or task overlap. Let $f_{\hat{\theta}}(z)$ denote the representation of an input z for all $z \in \mathbb{D}$. We use a kernel matrix $\mathbf{K} : \mathbb{D} \times \mathbb{D} \rightarrow \mathbb{R}$ of size $n \times n$ to measure similarity between representations, where $\mathbf{K}(z_i, z_j) = \langle f_{\hat{\theta}}(z_i), f_{\hat{\theta}}(z_j) \rangle$ and $\langle \cdot, \cdot \rangle$ is the inner product. Representation similarity between two models is often evaluated via kernel matrix comparison through a technique known as Centered Kernel Alignment (CKA) [29, 28]. Other common metrics include nearest-neighbor scores [28], mutual KNN [22], and SVCCA [49]. We use implementations of these from the codebase of [22], and report CKA in our main results (§5) due to its widespread in both vision and language models [22, 27]. Additional metrics are evaluated in the Appendix.

Implementation of splitting methods. For both splitting methods, we experiment with 3 training paradigms. We train image classifiers on CIFAR-10, CIFAR-100, and TinyImagenet; a VAE on CIFAR-10; and small language models on Shakespeare and TinyStories. We evaluate the representational similarity of models on both in-distribution (e.g. test set of training data) and out-of-distribution (e.g. unseen in training) datasets since similarity between models do not transfer uniformly from one dataset to another [8]. For image classifiers and the VAE, we use two popular datasets (MNIST [13] and SVHN [43]) as OOD datasets. For language data with dataset overlap, we train with either Shakespeare or TinyStories and used WikiText [35] as the OOD dataset; language models with task overlap are trained with three randomly chosen datasets in Table 2. For each training dataset, we train 10 pairs of models using 10 different seeds for image data (6 for text) and evaluate the representational similarity for model pairs on both in-distribution and OOD data.

Dataset splitting implementation. For image classifiers, dataset partitions P are the classes of the training dataset, while for language models, partitions are different blocks of texts—e.g. a tokenized text corpus divided into 80 evenly-sized blocks, with each block assigned randomly to one of D_1, D_2 . We experiment with dataset overlap proportions α ranging from 0.0 to 1.0.

Task splitting implementation. As described in §4.2, we have two methods of controlling task overlap. The first, **(1) task splitting with increasing dataset overlap** leverages the same datasets as in our

dataset splitting but changes the number of overlapping classes. The second method, **(2) task splitting with constant dataset overlap**, only works with the ColorShapeDigit800K dataset.

For task splitting method (1), we experiment with task overlap levels ranging from 0.0 to 1.0 and evaluate models on both in-distribution and OOD data as in the dataset splitting approach. For task overlap experiments with text models, we construct overlapping datasets by combining multiple text corpora, rather than simply splitting one dataset between two models. In our case, each dataset includes up to three three corpora, meaning the models see text from different writing styles during training. The task splitting is controlled by the number of overlapping corpora across the two models’ datasets. Therefore, we use the following terms for OOD data in the text splitting experiments: **common** = corpora used by both models during training; **OOD (one model)** = corpora seen by only one model; **OOD (both models)** = corpora not seen by either model.

For task splitting method (2), in which we only trained models on ColorShapeDigit800K, we used CIFAR-10, MNIST, and SVHN as OOD datasets to keep the evaluation consistent across all image experiments. Overlap levels 1, 2, 3 correspond to task overlap $\alpha = 0, 0.5, 1$, respectively.

5 Experimental Results

We experiment with dataset and task splitting methods on a variety of models and report results below. Overall, we find that increase both task and dataset overlap drive higher representation alignment between models, and that combining these two (as is done in our “task overlap with increasing dataset overlap” experiments) produces the strongest trend.

5.1 Effect of dataset overlap on representation similarity

Our experiments vary the amount of training data overlap while holding all other variables (dataset size, task, model architecture) constant. We report CKA scores between models with varying levels of dataset overlap in Figure 4. As this figure shows, there is a positive trend across different model types and modalities for both in-distribution and out-of-distribution testing: when datasets overlap more, the CKA score steadily rises for both in-distribution and out-of-distribution testing data. This is further supported by our linear regression analysis, which shows that experiments consistently yielded positive slope and high R^2 values. There are a few exceptions within the VAE results, but we hypothesize that the small capacity of the VAE architecture we chose limited its ability to learn rich representations of the data, reducing trend strength. Despite this anomaly, the consistent trend suggests that training data overlap drives representational alignment.

We hypothesize that the difference between the CKA scores given to in-distribution and out-of-distribution testing data points is because in-distribution test points more closely matches the training data which lead to more consistent feature representations. On the other hand, out-of-distribution test data has greater variability in the models’ representation.

5.2 Effect of task overlap on representation similarity

Here, we evaluate our two different methods of task splitting. First, we consider method (1), task splitting with increasing dataset overlap, which closely mirrors the setup of our dataset splitting experiments. Then, we analyze method (2), task splitting with constant dataset overlap, which eliminates the possible confounding variable of varying dataset size at each task split.

(1) Task splitting with increasing dataset overlap. In this first approach where both dataset and task overlap simultaneously increase, we observe a positive correlation between task overlap and CKA for both in-distribution and OOD test data as shown in Figure 5. The only exception to this trend is for the evaluation of in-distribution datasets for image classifier models (ResNet18 - CIFAR-100 and Resnet 18 - TinyImagenet). Models for these two datasets learn more aligned representations on in-distribution data when α is *lower*. To understand this, we visualize differences in the latent space representations via TSNE [61] for models trained with small ($\alpha = 0.2$) and large ($\alpha = 0.8$) task overlap. As Figure 10 shows, latent representations at $\alpha = 0.8$ and 0.2 both look similar, but the spread of features is much larger at $\alpha = 0.8$ ($[-95, +95]$ for both x, y dimensions) than at $\alpha = 0.2$ ($[-50, +50]$ for both x, y). This larger feature range, attributable to the larger variety of classes the

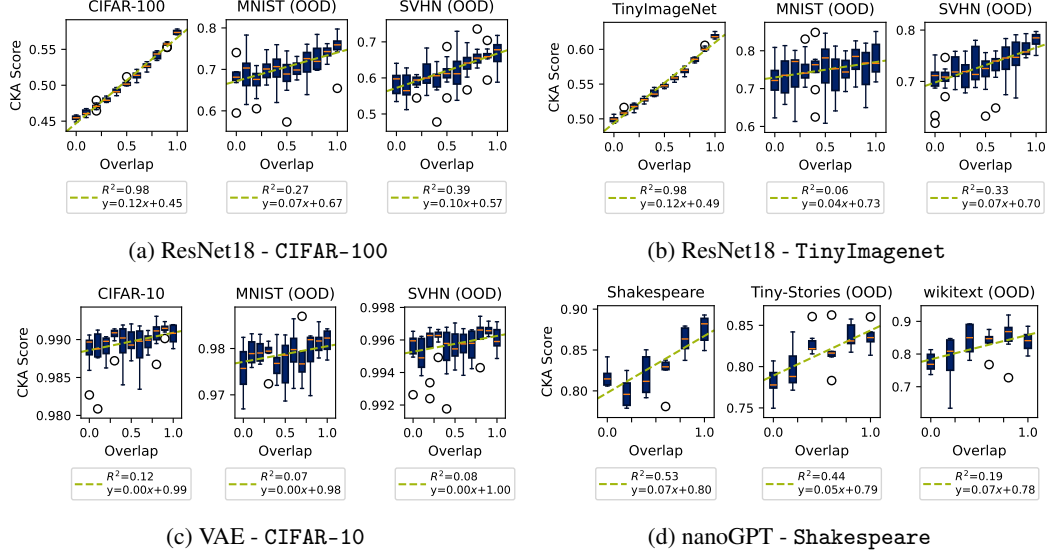


Figure 4: **Higher dataset overlap is positively correlated with higher representational similarity across the models we evaluate.** We report CKA scores between models with varying dataset overlap, evaluating on both in-distribution and OOD test data as described in §4.3.

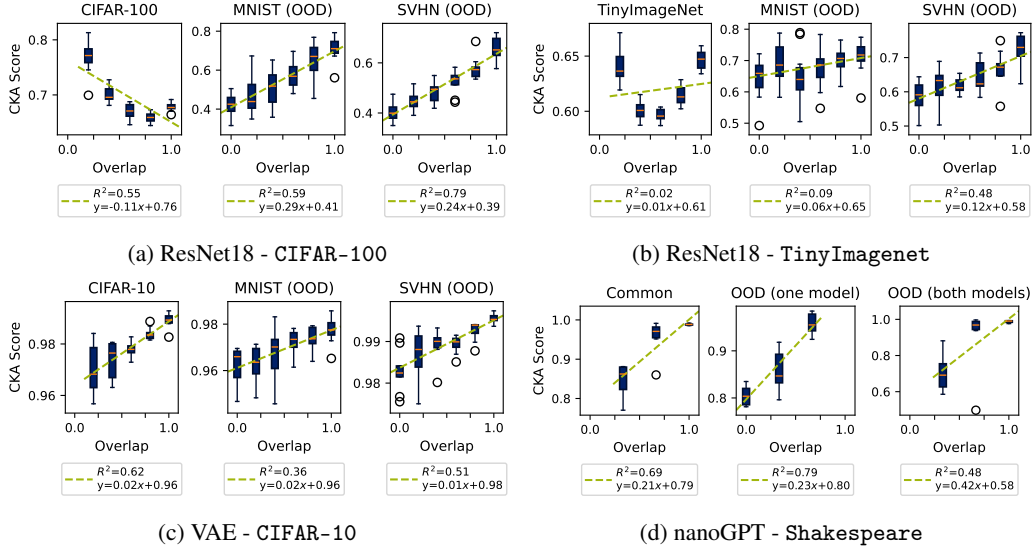


Figure 5: **Higher task overlap is positively correlated with higher representational similarity across the models we evaluate.** Results for task splitting method (1), in which dataset and task overlap increase together. We report CKA scores between models with varying task overlap, evaluating on both in-distribution and OOD test data as described in §4.3.

model processes for higher α , induces larger absolute differences in the feature space at evaluation, explaining the lower CKA at higher task overlap.

(2) Task splitting with constant data overlap. Although the first task splitting approach maintains consistency with the dataset splitting in terms of datasets and models evaluated, it introduces a confounding variable because dataset overlap increases as task overlap increases. Therefore, we isolate the effect of scaling task overlap through experiments on ColorShapeDigit800K, as described in §4.3. Results from these experiments are shown in Figure 6. We find that, even when images in D_1 and D_2 are identical, increased task overlap positively correlates with increased CKA similarity scores in the models we evaluate. Linear regression models fit to these data have a strong positive

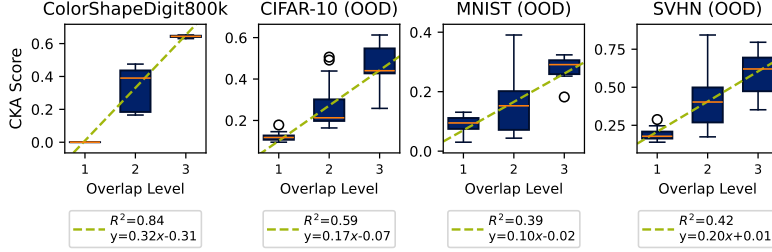


Figure 6: **Increasing task overlap with constant data overlap positively correlates with representational similarity.** Results for task splitting method (2). We report CKA scores for ResNet18 models trained on different overlap levels of ColorShapeDigit800K, as described in §4.3.

slope and reasonable R^2 values. These results empirically show that shared tasks among models, independent of data overlap, drive representational alignment.

5.3 Comparing the effects of dataset and task splitting on representational similarity

Finally, we evaluate which of our overlap methods—dataset alone, task alone, or dataset and task together—most strongly influences downstream representational similarity. To measure this, we use mutual information (MI) [53], an information-theoretic measure that quantifies the amount of shared information between two random variables. We compute the weighted mean mutual information for each overlap setting, where each model architecture evaluated contributes equally. Results are shown in Table 3. In this table, “task overlap” refers to experiments with ColorShapeDigit800K in which we vary task while holding dataset constant, while “task + dataset overlap” refers to experiments in which task and dataset overlap increase together.

Table 3: **Mutual information between dataset/task overlap and representational similarity is highest when both dataset and task overlap.** We report average mutual information between overlap and CKA metric across overlap types, weighted by model architecture. “Task overlap” refers to task splitting method (2) with ColorShapeDigit800K, while “task + dataset overlap” refers to task splitting method (1).

	Dataset Overlap	Task Overlap	Task + Dataset Overlap
Mutual Information	0.360	0.566	0.747

As Table 3 shows, the dataset and task overlap combined method has the highest MI score. This indicates that datasets with many shared characteristics (e.g. shared data points and task objectives) yield models with the most similar feature representations.

6 Discussion

Our work provides the first empirical investigation of potential *causes* of observed representational similarity in models. Through a broad empirical study, we find that both task and data overlap in model training data drive downstream representational similarity in models, and that combining these yields the highest effect. Here, we discuss broader implications and limitations of our work.

Broader impacts. Today’s large-scale AI models, particularly generative models, are often trained on overlapping datasets (§3.1) for similar purposes, e.g. serving as general purpose chatbots. Our findings that dataset and task overlap drive model similarity then suggest these models may have unexpectedly similar feature space representations. Recent work has surfaced concerns about how feature space alignment between models could result in homogeneous model behaviors. For example, Wenger and Kenett [63] showed that a broad set of generative AI models returns a narrow set of responses—much narrower than human responses—when responding to creative prompts. Homogeneity in AI models, in creative domains and beyond, could negatively impact AI users, who may find their AI-influenced behaviors unexpectedly narrowed and/or driven towards those of other AI users (e.g. [47]).

Limitations and future work. Our work has several limitations. First, we primarily use CKA to measure representational similarity. Prior work has pointed out downsides of CKA relative to other

metrics [2, 57]. CKA scores are also difficult to interpret—it has a maximum theoretical value of 1, but there is no established threshold for what score indicates strong alignment between models. Second, the size of models with which we experiment is limited due to compute constraints. This prevents us from making statements about how dataset and task overlap might affect similarity of today’s production-scale AI models. Third, we only compare models with the same architecture to avoid introducing confounding variables in our analysis, but future work could design controlled experiments to address this. Finally, we consider two possible factors affecting model similarity, but other factors could exist, leaving much room for future exploration.

References

- [1] Marah Abdin, Jyoti Aneja, Sebastien Bubeck, Caio César Teodoro Mendes, Weizhu Chen, et al. Phi-2: The surprising power of small language models, 2023. <https://www.microsoft.com/en-us/research/blog/phi-2-the-surprising-power-of-small-language-models/>.
- [2] Yamini Bansal, Preetum Nakkiran, and Boaz Barak. Revisiting model stitching to compare neural representations. *Proceedings of NeurIPS*, 34:225–236, 2021.
- [3] Rishi Bommasani, Drew A. Hudson, Ehsan Adeli, Russ Altman, Simran Arora, et al. On the opportunities and risks of foundation models, 2022. <https://arxiv.org/abs/2108.07258>.
- [4] Tom B Brown. Language models are few-shot learners. *arXiv preprint arXiv:2005.14165*, 2020. <https://arxiv.org/abs/2005.14165>.
- [5] William N. Caballero and Phillip R. Jenkins. On large language models in national security applications, 2024. <https://arxiv.org/abs/2407.03453>.
- [6] Jang Hyun Cho and Bharath Hariharan. On the efficacy of knowledge distillation. In *Proceedings of the IEEE/CVF international conference on computer vision*, pages 4794–4802, 2019.
- [7] Aakanksha Chowdhery, Sharan Narang, Jacob Devlin, Maarten Bosma, Gaurav Mishra, et al. Palm: Scaling language modeling with pathways. *Journal of Machine Learning Research*, 24(240):1–113, 2023.
- [8] Laure Ciernik, Lorenz Linhardt, Marco Morik, Jonas Dippel, Simon Kornblith, et al. Training objective drives the consistency of representational similarity across datasets, 2024. <https://arxiv.org/abs/2411.05561>.
- [9] Mert Cobanov. cobanov/shakespeare-dataset, 6 2022. <https://github.com/cobanov/shakespeare-dataset>.
- [10] Common Crawl. Common Crawl - Open Repository of Web Crawl Data., 2025. <https://commoncrawl.org/>.
- [11] DeepSeek-AI, Daya Guo, Dejian Yang, Haowei Zhang, Junxiao Song, et al. Deepseek-r1: Incentivizing reasoning capability in llms via reinforcement learning, 2025. <https://arxiv.org/abs/2501.12948>.
- [12] Jia Deng, Wei Dong, Richard Socher, Li-Jia Li, Kai Li, and Li Fei-Fei. Imagenet: A large-scale hierarchical image database. In *Proceedings of the IEEE/CVF international conference on computer vision*, pages 248–255. Ieee, 2009.
- [13] Li Deng. The mnist database of handwritten digit images for machine learning research. *IEEE Signal Processing Magazine*, 29(6):141–142, 2012.
- [14] Amil Dravid, Yossi Gandelsman, Alexei A. Efros, and Assaf Shocher. Rosetta neurons: Mining the common units in a model zoo, 2023. <https://arxiv.org/abs/2306.09346>.
- [15] Ronen Eldan and Yuanzhi Li. Tinstories: How small can language models be and still speak coherent english?, 2023. <https://arxiv.org/abs/2305.07759>.
- [16] Robert Geirhos, Kristof Meding, and Felix A Wichmann. Beyond accuracy: quantifying trial-by-trial behaviour of cnns and humans by measuring error consistency. *Proceedings of NeurIPS*, 33:13890–13902, 2020.
- [17] Wes Gurnee, Theo Horsley, Zifan Carl Guo, Tara Rezaei Kheirkhah, Qinyi Sun, et al. Universal neurons in gpt2 language models. *arXiv preprint arXiv:2401.12181*, 2024. <https://arxiv.org/abs/2401.12181>.
- [18] Guy Hacohen, Leshem Choshen, and Daphna Weinshall. Let’s agree to agree: Neural networks share classification order on real datasets. In *Proceedings of International Conference on Machine Learning*, pages 3950–3960. PMLR, 2020.
- [19] Shanshan Han, Qifan Zhang, Yuhang Yao, Weizhao Jin, Zhaozhuo Xu, et al. Llm multi-agent systems: Challenges and open problems, 2024. <https://arxiv.org/abs/2402.03578>.
- [20] Kaiming He, Xiangyu Zhang, Shaoqing Ren, and Jian Sun. Deep residual learning for image recognition, 2015. <https://arxiv.org/abs/1512.03385>.
- [21] Katherine L. Hermann and Andrew K. Lampinen. What shapes feature representations? exploring datasets, architectures, and training, 2020. <https://arxiv.org/abs/2006.12433>.

- [22] Minyoung Huh, Brian Cheung, Tongzhou Wang, and Phillip Isola. The platonic representation hypothesis, 2024. <https://arxiv.org/abs/2405.07987>.
- [23] Jared Kaplan, Sam McCandlish, Tom Henighan, Tom B Brown, Benjamin Chess, et al. Scaling laws for neural language models. *arXiv preprint arXiv:2001.08361*, 2020. <https://arxiv.org/abs/2001.08361>.
- [24] Karnika Kapoor. Chars74k, 2021. <https://www.kaggle.com/datasets/karnikakapoor/digits>.
- [25] Andrej Karpathy. nanogpt: The simplest, fastest repository for training/finetuning medium-sized gpts. <https://github.com/karpathy/nanoGPT>, 2023.
- [26] Diederik P. Kingma and Max Welling. An introduction to variational autoencoders. *Foundations and Trends® in Machine Learning*, 12(4):307–392, 2019. <http://dx.doi.org/10.1561/22000000056>.
- [27] Max Klabunde, Mehdi Ben Amor, Michael Granitzer, and Florian Lemmerich. Towards measuring representational similarity of large language models, 2023. <https://arxiv.org/abs/2312.02730>.
- [28] Max Klabunde, Tobias Schumacher, Markus Strohmaier, and Florian Lemmerich. Similarity of neural network models: A survey of functional and representational measures. *ACM Computing Surveys*, April 2025. <http://dx.doi.org/10.1145/3728458>.
- [29] Simon Kornblith, Mohammad Norouzi, Honglak Lee, and Geoffrey Hinton. Similarity of neural network representations revisited, 2019. <https://arxiv.org/abs/1905.00414>.
- [30] Alex Krizhevsky. Learning multiple layers of features from tiny images. pages 32–33, 2009. <https://www.cs.toronto.edu/~kriz/learning-features-2009-TR.pdf>.
- [31] Yixuan Li, Jason Yosinski, Jeff Clune, Hod Lipson, and John Hopcroft. Convergent learning: Do different neural networks learn the same representations?, 2016. <https://arxiv.org/abs/1511.07543>.
- [32] Grace W. Lindsay, Josh Merel, Tom Mscis-Flogel, and Maneesh Sahani. Divergent representations of ethological visual inputs emerge from supervised, unsupervised, and reinforcement learning, 2022. <https://arxiv.org/abs/2112.02027>.
- [33] Jun Ma, Yuting He, Feifei Li, Lin Han, Chenyu You, et al. Segment anything in medical images. *Nature Communications*, 15(1), January 2024. <http://dx.doi.org/10.1038/s41467-024-44824-z>.
- [34] Johannes Mehrer, Courtney J Spoerer, Nikolaus Kriegeskorte, and Tim C Kietzmann. Individual differences among deep neural network models. *Nature communications*, 11(1):5725, 2020.
- [35] Stephen Merity, Caiming Xiong, James Bradbury, and Richard Socher. Pointer sentinel mixture models, 2016. <https://arxiv.org/abs/1609.07843>.
- [36] Ari S. Morcos, Maithra Raghu, and Samy Bengio. Insights on representational similarity in neural networks with canonical correlation, 2018. <https://arxiv.org/abs/1806.05759>.
- [37] Luca Moschella, Valentino Maiorca, Marco Fumero, Antonio Norelli, Francesco Locatello, and Emanuele Rodolà. Relative representations enable zero-shot latent space communication. *arXiv preprint arXiv:2209.15430*, 2022. <https://arxiv.org/abs/2209.15430>.
- [38] Behzad Naderalvojoud and Tina Hernandez-Boussard. Improving machine learning with ensemble learning on observational healthcare data. In *Proceedings of the AMIA Annual Symposium*, volume 2023, page 521, 2024.
- [39] Nam Pham. tiny-textbooks (revision 14de7ba), 2023. <https://huggingface.co/datasets/nampdn-ai/tiny-textbooks>.
- [40] nampdn ai. Tiny codes dataset, 2024. <https://huggingface.co/datasets/nampdn-ai/tiny-codes>.
- [41] nampdn ai. Tiny webtext dataset, 2024. <https://huggingface.co/datasets/nampdn-ai/tiny-webtext>.
- [42] Humza Naveed, Asad Ullah Khan, Shi Qiu, Muhammad Saqib, Saeed Anwar, et al. A comprehensive overview of large language models, 2024. <https://arxiv.org/abs/2307.06435>.

- [43] Yuval Netzer, Tao Wang, Adam Coates, Alessandro Bissacco, Bo Wu, and Andrew Y. Ng. Reading digits in natural images with unsupervised feature learning. In *NIPS Workshop on Deep Learning and Unsupervised Feature Learning 2011*, 2011. http://ufldl.stanford.edu/housenumbers/nips2011_housenumbers.pdf.
- [44] Thao Nguyen, Maithra Raghu, and Simon Kornblith. Do wide and deep networks learn the same things? uncovering how neural network representations vary with width and depth, 2021. <https://arxiv.org/abs/2010.15327>.
- [45] Beatrix Miranda Ginn Nielsen, Luigi Gresele, and Andrea Dittadi. Challenges in explaining representational similarity through identifiability. In *UniReps: 2nd Edition of the Workshop on Unifying Representation and Abstractions in Neural Models*, 2024.
- [46] Adam Paszke, Sam Gross, Francisco Massa, Adam Lerer, James Bradbury, et al. Pytorch: An imperative style, high-performance deep learning library. *Advances in Neural Information Processing Systems*, 33, 2019.
- [47] Andrew J Peterson. Ai and the problem of knowledge collapse. *AI & SOCIETY*, pages 1–21, 2025.
- [48] Mary Phuong and Christoph Lampert. Towards understanding knowledge distillation. In *Proceedings of the International conference on machine learning*, pages 5142–5151. PMLR, 2019.
- [49] Maithra Raghu, Justin Gilmer, Jason Yosinski, and Jascha Sohl-Dickstein. Svcca: Singular vector canonical correlation analysis for deep learning dynamics and interpretability, 2017. <https://arxiv.org/abs/1706.05806>.
- [50] Tilman R  uker, Anson Ho, Stephen Casper, and Dylan Hadfield-Menell. Toward transparent ai: A survey on interpreting the inner structures of deep neural networks. In *Proceedings of IEEE Conference on Secure and Trustworthy Machine Learning (satml)*, pages 464–483. IEEE, 2023.
- [51] rivaldo. Geometric shapes - mathematics, 2022. <https://www.kaggle.com/datasets/reevald/geometric-shapes-mathematics>.
- [52] Geoffrey Roeder, Luke Metz, and Durk Kingma. On linear identifiability of learned representations. In *Proceedings of the International Conference on Machine Learning*, pages 9030–9039. PMLR, 2021.
- [53] Brian C. Ross. Mutual information between discrete and continuous data sets. *PLOS ONE*, 9(2):1–5, 02 2014.
- [54] Karsten Roth, Lukas Thede, Almut Sophia Koepke, Oriol Vinyals, Olivier H  naff, et al. Fantastic gains and where to find them: On the existence and prospect of general knowledge transfer between any pretrained model, 2024. <https://arxiv.org/abs/2310.17653>.
- [55] Shawn Shan, Emily Wenger, Jiayun Zhang, Huiying Li, Haitao Zheng, and Ben Y Zhao. Fawkes: Protecting privacy against unauthorized deep learning models. In *Proceedings of the 29th USENIX security symposium (USENIX Security 20)*, pages 1589–1604, 2020.
- [56] Ethan Steinberg, Ken Jung, Jason A. Fries, Conor K. Corbin, Stephen R. Pfohl, et al. Language models are an effective patient representation learning technique for electronic health record data, 2020. <https://arxiv.org/abs/2001.05295>.
- [57] Iliia Sucholutsky, Lukas Muttenthaler, Adrian Weller, Andi Peng, Andreea Bobu, et al. Getting aligned on representational alignment, 2024. <https://arxiv.org/abs/2310.13018>.
- [58] Jamba Team, Barak Lenz, Alan Arazi, Amir Bergman, Avshalom Manevich, Barak Peleg, Ben Aviram, Chen Almagor, Clara Fridman, Dan Padnos, et al. Jamba-1.5: Hybrid transformer-mamba models at scale. *arXiv preprint arXiv:2408.12570*, 2024. <https://arxiv.org/abs/2408.12570>.
- [59] Damien Teney, Armand Mihai Nicolicioiu, Valentin Hartmann, and Ehsan Abbasnejad. Neural redshift: Random networks are not random functions. In *Proceedings of the IEEE/CVF Conference on Computer Vision and Pattern Recognition*, pages 4786–4796, 2024.
- [60] Hugo Touvron, Thibaut Lavril, Gautier Izacard, Xavier Martinet, Marie-Anne Lachaux, Timoth  e Lacroix, Baptiste Rozi  re, Naman Goyal, Eric Hambro, Faisal Azhar, et al. Llama: Open and efficient foundation language models. *arXiv preprint arXiv:2302.13971*, 2023. <https://arxiv.org/abs/2302.13971>.

- [61] Laurens van der Maaten and Geoffrey Hinton. Visualizing data using t-SNE. *Journal of Machine Learning Research*, 9:2579–2605, 2008.
- [62] Xinyi Wang, Jianteng Peng, Sufang Zhang, Bihui Chen, Yi Wang, et al. A survey of face recognition, 2022. <https://arxiv.org/abs/2212.13038>.
- [63] Emily Wenger and Yoed Kenett. We’re different, we’re the same: Creative homogeneity across llms. *arXiv preprint arXiv:2501.19361*, 2025. <https://arxiv.org/abs/2501.19361>.
- [64] Yanzhao Wu, Ling Liu, Zhongwei Xie, Ka-Ho Chow, and Wenqi Wei. Boosting ensemble accuracy by revisiting ensemble diversity metrics. In *Proceedings of the IEEE/CVF Conference on Computer Vision and Pattern Recognition*, pages 16469–16477, 2021.

7 Appendix

Table 4: **Hyperparameter configurations across models and datasets.** We take the ResNet18 architecture directly from PyTorch [46] with modifications specified below.

Setting	Hyperparameter	CIFAR-10 & CIFAR-10 ResNet18	TinyImageNet (Dataset Split) ResNet18	TinyImageNet (Task Split) ResNet18	VAE	nanoGPT
Base Parameters	Learning rate	0.5	0.5	0.05	1.00E-03	1.00E-03
	Epochs/Iterations	70	100	90	30	5000
	Batch size	512	256	256	256	16
Optimization	Optimizer	SGD	SGD	SGD	Adam	AdamW
	Momentum	0.9	0.9	0.9	-	-
	Weight decay	5.00E-04	5.00E-04	1.00E-04	1.00E-05	1.00E-01
	Label smoothing	0.1	0.1	0.1	-	-
	LR scheduler	Cyclic	Cyclic	Cyclic	None	Cosine w/warmup
	LR peak epoch	10	10	5	-	-
Architecture	Model type	ResNet18	ResNet18	ResNet18	VAE	Transformer
	Input size	32×32	64×64	64×64	28×28	-
	First conv	3×3	7×7	3×3	4×4	-
	Output features	100	200	200	-	-
Special Features	Regularization	-	Dropout (0.5)	-	KL div ($\beta=1$)	Dropout (0.2)
	Gradient accumulation	No	No	No	No	Yes (8 steps)
	Context length	-	-	-	-	256 tokens

Table 5: **Accuracy of trained ResNet18 models.** The mean accuracy and standard deviation of the accuracy over 10 seeds is given for each splitting method. The task splitting experiments use our dataset (ColorShapeDigit800k) for training and evaluation.

Dataset	Dataset Overlap	Task Overlap	Task + Dataset Overlap
CIFAR-10	92.26 \pm 0.20	NA	96.82 \pm 1.36
CIFAR-100	68.36 \pm 0.34	NA	80.73 \pm 1.70
TinyImageNet	45.99 \pm 0.32	NA	60.75 \pm 1.95
P1: shape labels	NA	99.05 \pm 0.03	NA
P1: digit labels	NA	99.54 \pm 0.05	NA
P2: shape & color labels	NA	99.01 \pm 0.02	NA
P2: digit & color labels	NA	99.49 \pm 0.04	NA
P2: shape & digit labels	NA	98.66 \pm 0.03	NA
P3: shape, digit, & color labels	NA	98.53 \pm 0.05	NA

7.1 Comparison of representational similarity metrics

Here, we present the full results for all models evaluated on 7 major representational similarity metrics (from codebase of [22]) We include similarity metrics evaluated using OOD data from the original training distribution for task splitting method (1) experiments performed on ResNet and VAE (Figures 7a, 8a, 9a and 11a). For both task and dataset splitting, we always create two datasets of equal size and divide them into the same number of partitions, regardless of the value of α . Under task splitting, entire partitions are assigned to one dataset or the other. For $\alpha > 0$, this approach means some partitions from the original training distribution \mathbb{D} are excluded from both datasets (D_1 and D_2). Therefore, we use these excluded partitions as (OOD) data in our evaluations. We label OOD data as <dataset name> (OOD)—for example, CIFAR-10 (OOD)—to indicate that the data comes from the underlying data distribution \mathbb{D} but does not belong to any partition in $D_1 \cup D_2$.

7.1.1 Full ResNet Results

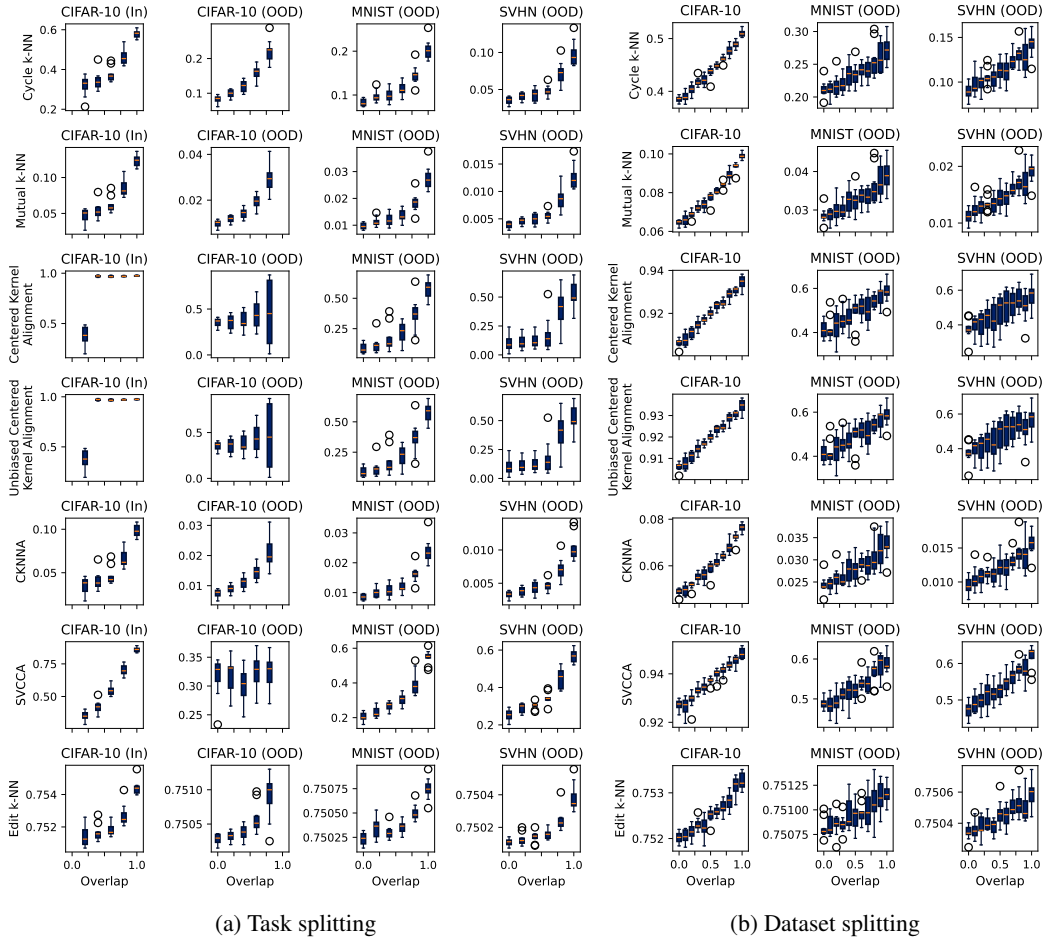


Figure 7: All similarity scores for task and dataset splitting (CIFAR-10). Representational similarity measured using metrics in [22] for ResNet under task and dataset splitting with error bars representing deviation across different splitting and training seeds.

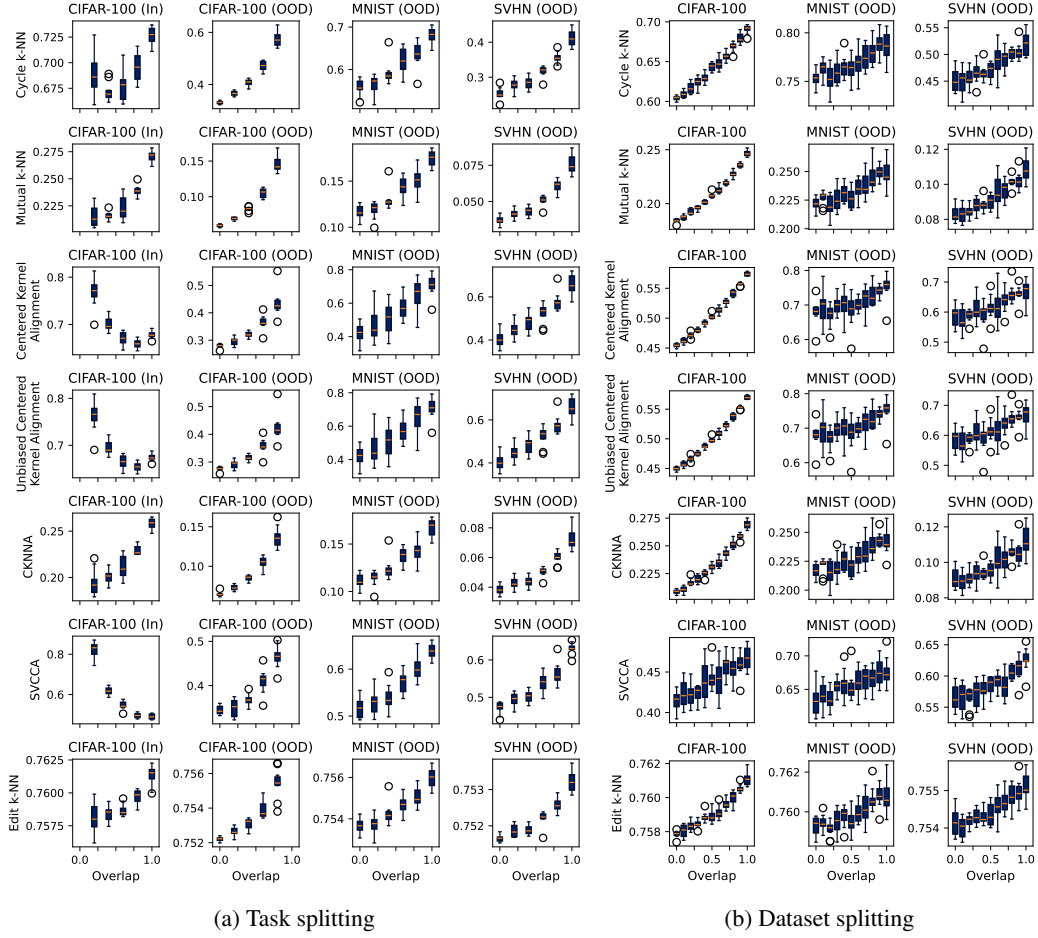


Figure 8: All similarity scores for task and dataset splitting (CIFAR-100). Representational similarity measured using metrics in [22] for ResNet under task and dataset splitting with error bars representing deviation across different splitting and training seeds.

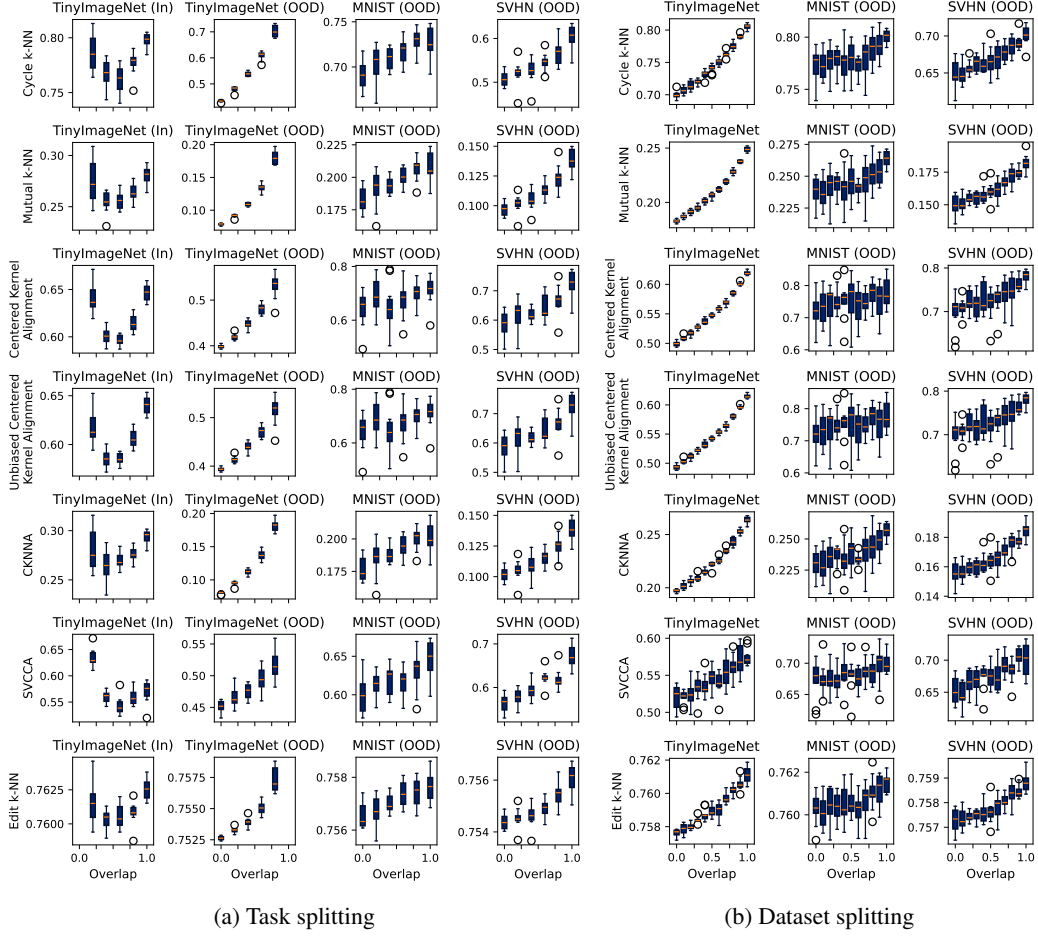


Figure 9: **All similarity scores for task and dataset splitting (TinyImageNet).** Representational similarity measured using metrics in [22] for ResNet under task and dataset splitting with error bars representing deviation across different splitting and training seeds.

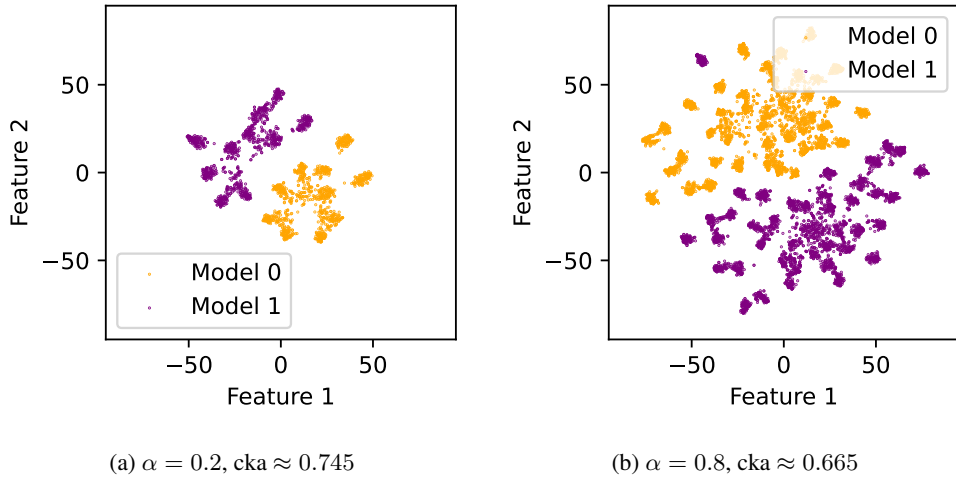


Figure 10: **TSNE visualizations for CIFAR-100 task overlap models.** Visualizations of latent space representations of in-distribution CIFAR-100 images (i.e., latent representations are produced using images in the test set found in the classes in $D_1 \cap D_2$) for $\alpha = 0.2$ and $\alpha = 0.8$. Dimension reduction is performed by TSNE [61].

7.1.2 Full VAE Results

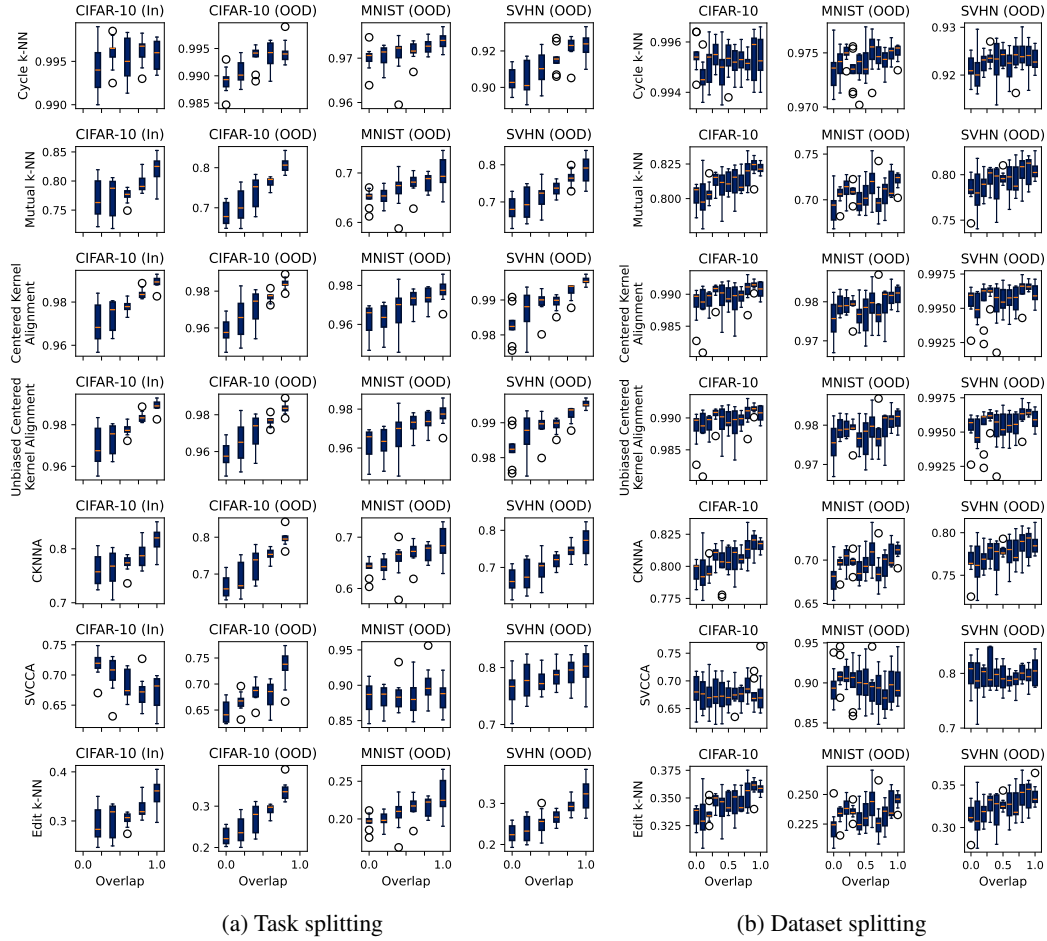


Figure 11: **All similarity scores for task and dataset splitting (CIFAR-10).** Representational similarity measured using metrics in [22] for VAE under task and dataset splitting with error bars representing deviation across different splitting and training seeds.

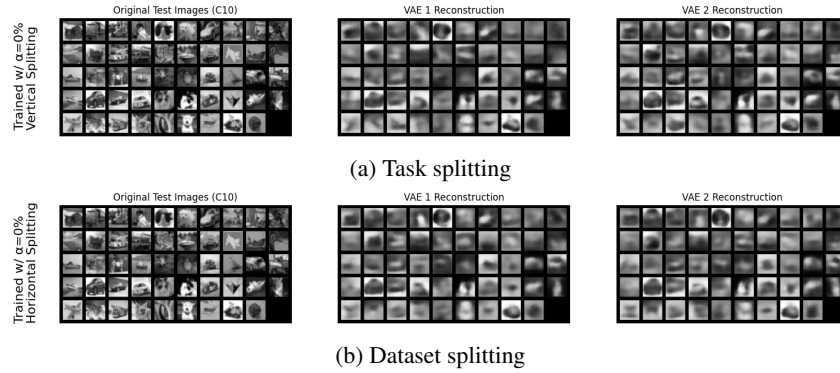


Figure 12: **Generated images.** Samples of generated images using VAE models trained on datasets generated using both task and dataset splitting (CIFAR-10).

7.1.3 Full nanoGPT Results

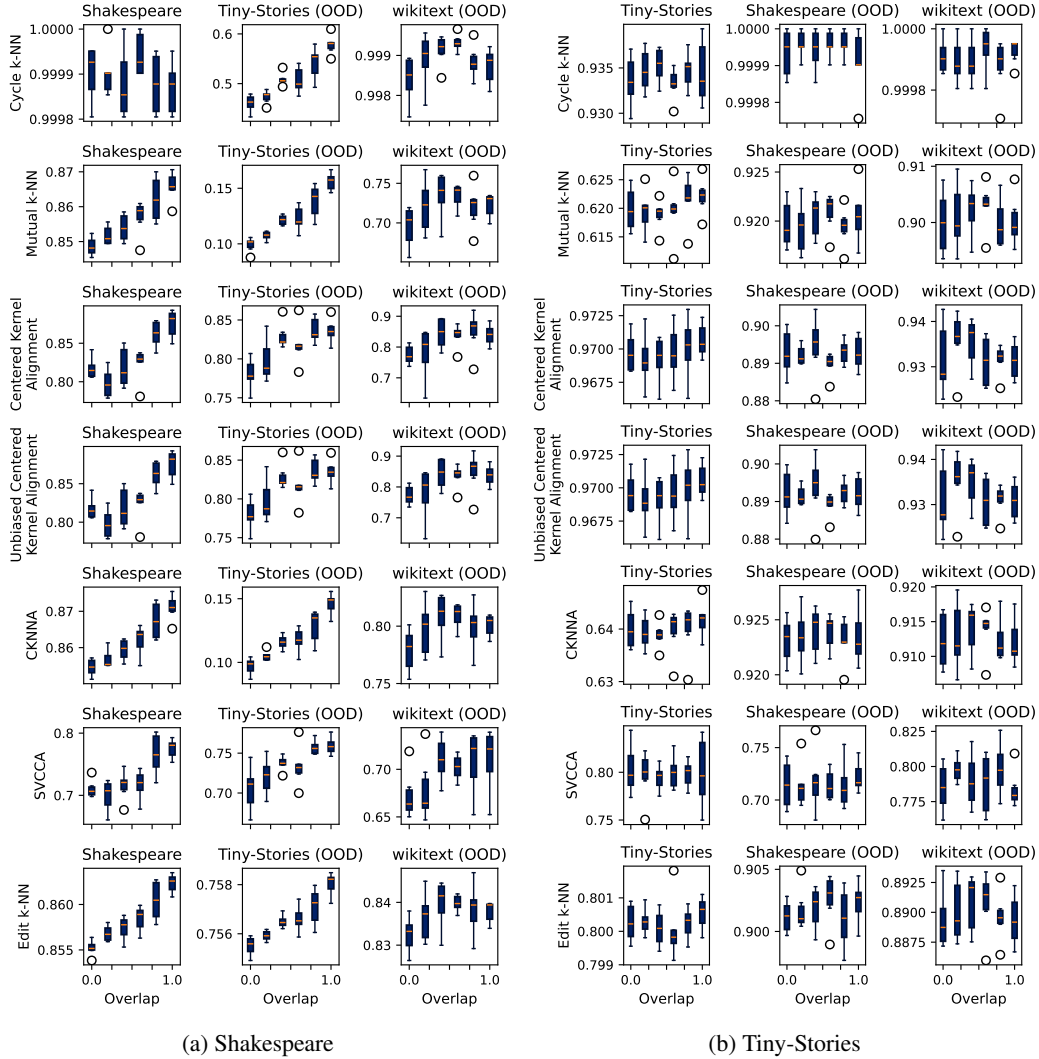


Figure 13: All similarity scores for dataset splitting (nanoGPT). Representational similarity measured using metrics in [22] for nanoGPT under dataset splitting with error bars representing deviation across different splitting and training seeds.

For all sample text, the starting prompt is Do you not hear.

Sample text generated by a Transformer trained on Tiny-Stories (dataset overlap):

Do you not hear this noise? It's dangerous. It's not for playing. It's dangerous."

Ben does not listen. He does not care about the noise. He says, "No, I don't want to see. It's just a noise. It's scary." He throws his gun at the dog. The dog runs away.

Sample text generated by a Transformer trained on Shakespeare (dataset overlap):

Do you not hear me, and your love,
I would not lose with your love.
[She exits.]

Scene 1

=====

[Flourish. Enter Polonius, Brutus, the stage.]

HAMLET

Away, the music. Enter Hamlet, Ophelia,
With all his good one another's life and night,

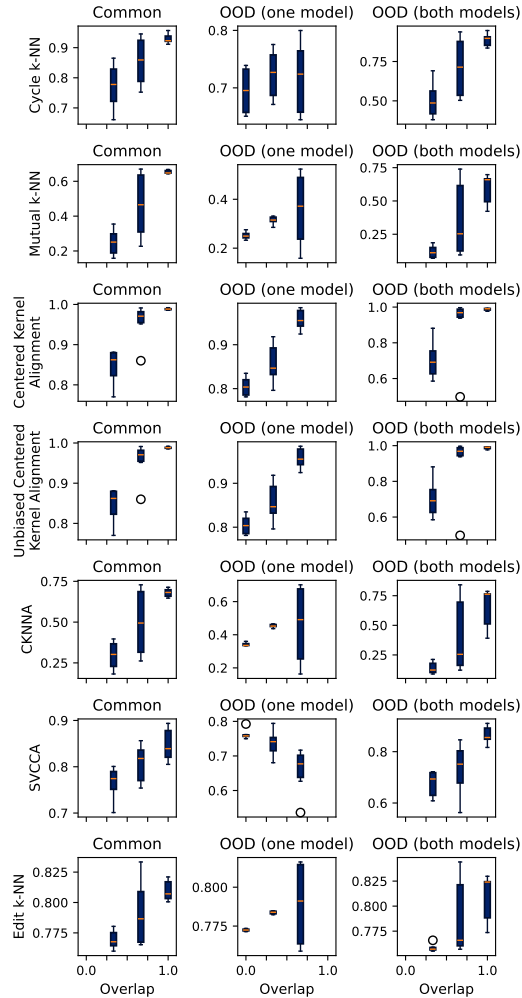


Figure 14: All similarity scores for task splitting (nanoGPT). Representational similarity measured using metrics in [22] for nanoGPT under task splitting with error bars representing deviation across different splitting and training seeds.

Sample text generated by a Transformer with a dataset constructed using task splitting:

Do you not hear anything about these symptoms within this study? (y/n): "

```
if answer == 'Y' or answer == 'y':
    print("How often do you experience symptoms such as cough, fever,
    difficulty breathing?")
    print("What types of symptoms do you have?")
    print("Are you within several hours of this day?")
    print("Do you have any questions about these symptoms?")
```

7.1.4 Full ColorShapeDigit800k Results

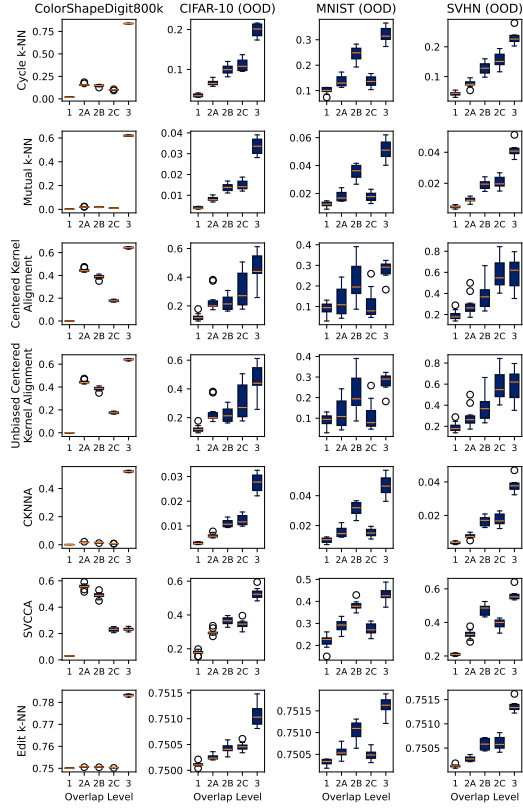


Figure 15: All similarity scores for task overlap while keeping dataset overlap constant (ResNet). Representational similarity measured using metrics in [22] for ResNet under different task overlap with constant dataset overlap with error bars representing deviation across different splitting and training seeds. Please refer to Table 1 for information on each overlap level.